IRIS AperTO

UNIVERSITÀ DEGLI STUDI DI TORINO

AperTO - Archivio Istituzionale Open Access dell'Università di Torino

Knock-down of synapsin alters cell excitability and action potential waveform by potentiating BK and voltage-gated Ca2+ currents in Helix serotonergic neurons

This is the author's manuscript

Original Citation:

Availability:

This version is available http://hdl.handle.net/2318/1531415 since 2016-12-02T17:58:44Z

Published version:

DOI:10.1016/j.neuroscience.2015.10.046

Terms of use:

Open Access

Anyone can freely access the full text of works made available as "Open Access". Works made available under a Creative Commons license can be used according to the terms and conditions of said license. Use of all other works requires consent of the right holder (author or publisher) if not exempted from copyright protection by the applicable law.

(Article begins on next page)

02 May 2026

IRIS AperTO

UNIVERSITÀ DEGLI STUDI DI TORINO

This Accepted Author Manuscript (AAM) is copyrighted and published by Elsevier. It is posted here by agreement between Elsevier and the University of Turin. Changes resulting from the publishing process - such as editing, corrections, structural formatting, and other quality control mechanisms - may not be reflected in this version of the text. The definitive version of the text was subsequently published in NEUROSCIENCE, 311, 2015, 10.1016/j.neuroscience.2015.10.046.

You may download, copy and otherwise use the AAM for non-commercial purposes provided that your license is limited by the following restrictions:

(1) You may use this AAM for non-commercial purposes only under the terms of the CC-BY-NC-ND license.

(2) The integrity of the work and identification of the author, copyright owner, and publisher must be preserved in any copy.

(3) You must attribute this AAM in the following format: Creative Commons BY-NC-ND license (http://creativecommons.org/licenses/by-nc-nd/4.0/deed.en), 10.1016/j.neuroscience.2015.10.046

The publisher's version is available at:
http://linkinghub.elsevier.com/retrieve/pii/S0306452215009653

When citing, please refer to the published version.

Link to this full text:
http://hdl.handle.net/2318/1531415

This full text was downloaded from iris - AperTO: https://iris.unito.it/

iris - AperTO

University of Turin's Institutional Research Information System and Open Access Institutional Repository

Knock-down of synapsin alters cell excitability and action potential waveform by potentiating BK and voltage-gated Ca^{2+} currents in *Helix* serotonergic neurons

Brenes Oscar[1,2], Vandael David H.F.[3,4,6], Carbone Emilio[3,4], Montarolo Pier Giorgio[1,5], Ghirardi Mirella[1,5]

1 Department of Neuroscience, Section of Physiology, University of Turin, Turin, Italy

2 Department of Physiology, School of Medicine, University of Costa Rica, San José, Costa Rica

3 Department of Drug Science, Lab of Cellular and Molecular Neuroscience, Turin, Italy

4 Nanostructured Interfaces and Surfaces Center, Turin, Italy

5 National Institute of Neuroscience, Turin, Italy

Corresponding author

O. Brenes. Department of Physiology, School of Medicine, University of Costa Rica, 2060, San José, Costa Rica. Tel: +506 2511 4391; Fax: +506 2511 4482; Email: oscar.brenes_g@ucr.ac.cr, oscar.brenesgarcia@edu.unito.it

Grant information

This work was supported by Grants from the Italian Ministry of the University and Research (PRIN 2009 grants to PGM) and Compagnia di San Paolo (to PGM and MG). Funding sources had no involvement in study design, or decision making about writing and submitting the article.

6 Author's present address

D.H.F. Vandael: Institute of Science and Technology Austria, Am Campus 1, Klosterneuburg, Austria

Abbreviations

AHP (After hyperpolarization)

AP (Action potential)

RRP (Readily releasable pool)

asRNA (antisense RNA)

Em (Resting membrane potential)

helSyn (*Helix* synapsin)

helSynKD (*Helix* synapsin knock-down)

IFF (Instantaneous firing frequency)

ISI (Interspike interval)

KO (Knock-out)

MFF (Mean firing frequency)

R_{in} (Input resistance)

SFA (Spike frequency adaptation)

Syn (Synapsin)

V_{th} (Voltage threshold)

s.e.m. (Standard error of the mean)

Abstract

Synapsins are an evolutionarily-conserved family of presynaptic proteins crucial for the fine-tuning of synaptic function. A large amount of experimental evidences has shown that the synapsins are involved in the development of epileptic phenotypes and several mutations in synapsin genes have been associated with epilepsy in humans and animal models. Synapsin mutations induce alterations in circuitry and neurotransmitter release, differentially affecting excitatory and inhibitory synapses, thus causing an excitation/inhibition imbalance in network excitability toward hyperexcitability that may be determinant with regard to the development of epilepsy. Another approach to investigate epileptogenic mechanisms is to understand how silencing synapsin affects cellular behavior of single neurons and is associated with the hyperexcitable phenotypes observed in epilepsy. Here, we examined the functional effects of antisense-RNA inhibition of synapsin expression in individually identified and isolated serotonergic cells of the *Helix* land snail. We found that *Helix* synapsin silencing increases cell excitability characterized by a slightly depolarized resting membrane potential, decreases the rheobase, reduces the threshold for action potential (AP) firing and increases the mean and instantaneous firing rates, with respect to control cells. The observed increase of Ca^{2+} and BK currents in synapsin-silenced cells seems to be related to changes in the shape of the AP waveform. These currents sustain the faster spiking in synapsin-deficient cells by increasing the after hyperpolarization and limiting the Na^{+} and Ca^{2+} channel inactivation during repetitive firing. This in turn speeds up the depolarization phase by reaching the AP threshold faster. Our results provide evidence that synapsin silencing increases intrinsic cell excitability associated with increased Ca^{2+} and Ca^{2+}-dependent BK currents in the absence of excitatory or inhibitory inputs.

Keywords

Synapsin; invertebrate neurons; cell excitability; calcium channels; BK channels.

Synapsins (Syns) are an evolutionarily conserved family of presynaptic proteins, crucial for the fine tuning of synaptic transmission and synaptic remodeling. Syn homologues have been found all across the metazoan tree, from Cnidaria to Vertebrata, with one single gene identified in invertebrates and three different genes (called SYN1, SYN2 and SYN3) described in mammals, all highly conserved and sharing similar modular structure (Cesca et al., 2010).

In addition to several roles of Syns in physiological neuronal functioning, increasing evidence indicates that these proteins are involved in epilepsy development (Li et al., 1995; Rosahl et al., 1995; Gitler et al., 2004; Etholm and Heggelund, 2009; Ketzef et al. 2011; Etholm et al., 2013). In mammals it has been shown that almost all single, double or triple Syn knock-out (KO) mice develop a severe epileptic phenotype induced by sensory stimulation (for review see Cesca et al., 2010 and Fassio et al., 2011a). In humans, several nonsense and missense Syn mutations associated with epilepsy, among other disorders, have been reported and characterized to some degree, for both SYN1 (García et al., 2004; Fassio et al., 2011b; Lignani et al., 2013, Giannandrea et al., 2013) and SYN2 genes (Cavalleri et al., 2007; Lakhan et al., 2010; Corradi et al., 2014).

The establishment of connections among neurons depends on the correct timing of neuronal development and Syn proteins are the main regulators of wiring the brain during development (Cesca et al., 2010). Several studies provided evidence that Syns play a fundamental role in the development of neurites (Ferreira et al. 1994; 1998, Kao et al., 2002), and in the formation, maintenance and rearrangements of synaptic contacts (Ferreira et al., 1998; Chin et al., 1995). It is also accepted that Syns modulate synaptic vesicle pools, modifying the readily releasable pool (RRP), the recycling pool, and the resting pool sizes (Humeau et al., 2001; Feng et al., 2002; Gitler et al., 2004; Gaffield and Betz, 2007; Chiappalone et al., 2009; Messa et al., 2010; Kile, 2010; Valtorta et al., 2011; Farisello et al., 2012; Orenbuch et al., 2012; Verstegen et al., 2014; Brenes et al., 2015). Epileptic disorders have been related with deficiencies in

Syn-regulated processes such as neurite outgrowth, synapse formation or neurotransmitter release. In fact, the development of epilepsy in Syn mutants has been associated with i) alterations of neurite outgrowth and synaptogenesis leading to abnormal circuitry during maturation (Cesca et al., 2010), and ii) modification of the synaptic vesicle pool mobility and release with consequent differential changes of the rate of neurotransmitter release in excitatory and inhibitory synapses, thus causing an excitation/inhibition imbalance in network excitability (Gitler et al., 2004; Baldelli et al., 2007; Chiappalone et al., 2009; Noebels et al., 2010; Pitkänen and Lukasiuk, 2011; Farisello et al., 2012; Lignani et al., 2013).

Progressive alterations of neuronal excitability observed in epileptic disorders may be due to the development of intrinsic changes at the cellular level, independent of excitatory and inhibitory inputs to the cells (Noebels 2003; Kandel et al., 2013). The aim of the present study is to investigate the effects of Syn silencing on the electrophysiological properties of isolated identified neurons completely deprived of their synaptic inputs. The neurons of the land snail *Helix* provide several advantages for this study since specific identifiable neurons can be isolated independently and cultured avoiding the effects of surrounding tissue or excitatory and inhibitory synaptic inputs (Ghirardi et al., 1996; Fiumara et al., 2001). These neurons also allow performing complex experimental manipulations such as plasmid intra-nuclear microinjection and provide a convenient genetic organization with a single Syn gene (Fiumara et al., 2007) that may be blocked by antisense RNA (asRNA) (Brenes et al., 2015). By injecting plasmids codifying constitutively expressed asRNA, Syn can be silenced in isolated single cells and cellular excitability can be analyzed, together with the ionic currents controlling cell excitability, widening our knowledge about the role of Syn in the development of alterations in neuronal excitability.

1. Experimental procedures

1.1. Materials

All chemicals and reagents used in this study were purchased from Sigma (Milan, Italy), unless stated otherwise.

1.2. Animals

Juvenile specimens of *Helix aspersa* land snails were provided by local breeders and maintained inactive at a temperature of 6 °C. Before experimental procedures, snails were kept in an active state for at least 16 h in a climatic chamber regulating temperature and humidity (20°C and 70% relative humidity). During the active period, snails were fed with lettuce and water *ad libitum*. During surgical procedures, the snails were always anesthetized and efforts were made to minimize the number and suffering of animals used, in accordance with Directive 2010/63/EU of the European Parliament and of the Council of 22 September 2010 on the protection of animals used for scientific purposes.

1.3. Cell Culture

Cell cultures were performed as previously described (Ghirardi et al., 1996). Briefly, the snails were anesthetized by the injection of isotonic $MgCl_2$ in the foot. Cerebral ganglia were surgically isolated and incubated for enzymatic digestion in protease type XIV in isotonic L15 medium (0.4 U/ml) at 34°C for 3 h. After digestion, the ganglia were washed two times in L15 medium and C1 neurons were individually isolated, identified by their position in the ganglia and their size. Neurons were isolated and transferred to dishes pretreated with 5 % bovine serum albumin to prevent cell-substrate adhesion. After 24 h floating neurons retracted their processes, forming spherical axon-reabsorbed somata (soma-configuration), as previously described (Fiumara et al., 2005). Then, floating somata were microinjected and gently manipulated according to the specific experimental requirements.

1.4. *Helix* synapsin knock-down

Standard recombinant DNA techniques were used to generate two different plasmids. The first one was the plasmid $pNEX_3$ containing EGFP sequence (pNEX-EGFP). In the second one, the DNA sequence corresponding to the 3' third of mRNA of helSyn (544 bp) was cloned in an inverted way in the $pNEX_3$ plasmid, depleted of EGFP (pNEX-helSynAS). Upon intra-nuclear microinjection these constructs lead to constitutive expression of EGFP protein or an asRNA against the final part of helSyn mRNA. Control cells were injected with the pNEX-EGFP. helSynKD cells were injected with both pNEX-helSynAS and pNEX-EGFP. Intra-nuclear microinjection was done with a glass electrode, with the tip filled with a solution containing the plasmids (1 µg/ml each), KCl (0.2 M) and Fast Green solution 0.2 % (p/v), and loaded using short pressure pulses (10-20 pulses, 2-10 psi) delivered through a pneumatic picopump (PV820, WPI) connected to the electrode holder. The injection procedure was monitored under visual and electrophysiological control and stopped when the nucleus was uniformly colored. Cells expressing the asRNA and control cells were analyzed by immunocytochemistry in order to estimate Syn protein presence. As we previously showed (Brenes et al., 2015), cells expressing the asRNA for 48 h and 72 h showed a marked decrease in Syn immunostaining, and only these cells were used for the electrophysiological experiments.

1.5. Electrophysiological recordings

Standard intracellular recording techniques were used in cultured cells under an inverted microscope (Eclipse TE200, Nikon Instruments, Tokyo, Japan) as previously described by Fiumara et al. (2005; 2007). Briefly, the cells were impaled with glass intracellular electrodes, filled with 2.5 M KCl (resistance ~10 MΩ). Signals were amplified by an Axoclamp 900A amplifier (Axon Instruments, Union City, CA, USA) in current clamp mode, digitally converted by means of a Digidata 1322A analog/digital converter (Axon Instruments) and monitored and recorded with Axoscope software (Axon Instruments) on a PC.

Ca^2+ and K^+ currents were recorded in whole cell patch configuration using a Multiclamp 700A amplifier (Axon Instruments, Union City, CA, USA) or an EPC-10 HEKA amplifier (HEKA-Elektronic, Germany) and recorded using Axoscope software or Pulse software, respectively. Borosilicate glass pipettes of 1-2 MΩ input resistance were filled with different intracellular solutions according to the experimental aim (Marcantoni et al. 2009). Series resistance of 3 to 5 MΩ was compensated by 50% before recording. For recording K^+ currents the intracellular solution was (in mM): 3 NaCl, 100 KCl, 1 $MgCl_2$, 10 HEPES, 5 EGTA, pH 7.4 (with KOH) while the extracellular solution was (in mM): 10 NaCl, 90 CholineCl, 5 KCl, 2 $CaCl_2$, 10 $MgCl_2$, 10 HEPES, pH 7.4 (with NaOH). For recording Ca^{2+} currents the intracellular solution was (in mM): 3 NaCl, 100 CsCl, 1 MgCl2, 10 HEPES, 5 EGTA, pH 7.4 (with CsOH) while the extracellular solution was (in mM): 105 TEACl, 2 $CaCl_2$, 10 $MgCl_2$, 10 HEPES, pH 7.4 (with CsOH). Due to the large capacitance of Helix neurons (~314 pF) the dynamic response of the voltage-clamp amplifier was slow at low negative voltages where Ca^{2+} and K^+ channel conductance was low but was sufficiently fast at positive potentials where Ca^{2+} and K^+ conductance reached maximal values (see Fig. 6A and 7A).
To fully inhibit BK currents, 1μM paxilline was added to the extracellular solution or the L15 medium (Marcantoni et al., 2010; Zhou and Lingle, 2014). The recorded traces were analyzed with Clampfit software (Axon Instruments) or Pulse software (HEKA-Elektronic). Fitting of gK versus V with a Boltzmann equation was performed using Origin software (Marcantoni et al., 2010).

1.6. Electrophysiological measurements

The rheobase was determined by applying a depolarizing stimulus of 50 ms and increasing intensity until the cell fired an action potential (AP) and the stimulation was repeated at least three times. Voltage threshold for AP firing (V_{th}) was determined as the voltage at which the upslope velocity of the AP increased rapidly. At least 10 APs of each cell were averaged and their membrane voltages were plotted against their first time derivative (dV/dt), resulting in a phase plane plot of the spike (Jenerick, 1963;

Vandael et al., 2012). The V_{th} was selected as the voltage at which dV/dt exceeded 3 times the standard deviation of all the preceding data points (Soto et al., 2000; Bailey et al., 2003). Input resistance (R_{in}) was calculated through quantification of changes in membrane voltage evoked by five depolarizing and five hyperpolarizing current injections of increasing amplitude. Voltage membrane was plotted as a function of injected current, and then values were fitted by linear relation, the slope of which is the R_{in} of the cell (Bailey et al., 2003).

For the AP waveform analysis we measured different variables (Fig. 1). The fast after hyperpolarization (AHP) was measured as the difference between the resting membrane potential (Em) before the stimulation and the minimum membrane voltage after the action potential. The decay time 90%-10% was the duration (in ms) of the repolarization between the 90% and the 10% of the total repolarization phase. The decay time constant (decay tau) correspond to the time elapsed after membrane voltage has fallen to 37% of the maximum voltage attained during the AP. Half-width was measured at half of the spike amplitude. AP amplitude was measured as the difference between the peak and the resting potential before the stimulation. The depolarizing phase was analyzed measuring the time elapsed from the beginning to the peak of the AP (time to peak) and measuring the maximal velocity achieved during the depolarization (maximum rise slope).

The mean firing frequency (MFF) was calculated with the number of APs fired by 500 ms depolarizing stimulations of 0.5, 1.0 and 1.5 nA. Instantaneous Firing Frequency during the 1.5 nA stimulations (IFF) was calculated as 1 / interspike interval (ISI). And, the Spike Frequency Adaptation (SFA) was estimated by the ratio between the first and the second ISI from the 1.5 nA stimulations (adaptation ratio).

1.7. Statistical analysis

Data were expressed as means ± s.e.m. Statistical analysis was performed using GraphPad Prism version 5 (GraphPad Software, San Diego, CA). Statistical significance between group means was assessed using Student's t-test or Welch

corrected t-test, both of two tails and ANOVA (one-way, two-way or repeated measures where appropriate) followed by the Bonferroni post-hoc test or Kruskal-Wallis test followed by Dunn's multiple comparison test. Significance levels were set at $P < 0.05$.

2. Results

2.1. Increased cellular excitability in Syn-silenced cells.

In order to block Syn synthesis we nuclearly microinjected a plasmid that codifies an asRNA complementary with *Helix* synapsin (helSyn) mRNA. Silencing efficacy was analyzed 48 and 72 h after asRNA expression by immunocytochemical analysis. Our knock-down strategy resulted in an almost 90% loss of Syn in the cellular varicosities (Brenes et al., 2015). As shown in Fig. 2A and B, Syn staining signal in the varicosities of *Helix* neurons was strongly decreased in helSynKD cells with respect to control cells. Since Syn deletion and mutation have been associated with the development of epileptic phenotypes and progressive alterations of neuronal excitability we decided to analyze the cellular excitability in Syn-silenced cells. Cell excitability was estimated by determining the Em, measuring the minimal current intensity necessary to evoke an action potential (rheobase), calculating the AP-threshold and characterizing the firing patterns as a function of the stimulus strength.

Helix Syn knock-down cells (helSynKD) showed a slightly depolarized resting potential (-49.9 ± 0.9 mV, n = 39), with respect to control cells (-53.1 ± 0.7 mV, n = 42) ($t_{(79)}$ = 2.7, P < 0.01) (Fig. 3A), and a 50 % smaller rheobase (0.62 ± 0.06 nA, n = 19 in helSynKD cells; vs 1.22 ± 0.08 nA, n = 28 in control cells) (Welch corrected $t_{(44)}$ = 5.76, P < 0.0001) (Fig. 3B).

Averaged APs were used for the phase plane plot analysis (Fig. 3C), membrane voltage was plotted against the first time derivative (dV/dt) and V_{th} was determined as the voltage at which the upslope velocity (dVdt) of the AP increased rapidly over baseline values (see Experimental procedures section). We observed a more negative V_{th} in helSynKD cells (-26.5 ± 1.0 mV, n = 26), with respect to control cells (-22.7 ± 1.4 mV, n = 21) ($t_{(45)}$ = 2.2, P < 0.05) (Fig. 3C, insert).

When the firing response to three different sustained (500 ms) depolarizing current injections was evaluated (Fig. 4A), helSynKD cells showed a greater number of AP fired, translated in a higher MFF at all current intensities tested (0.5 nA: 5.3 ± 0.4 Hz;

1.0 nA: 8.9 ± 0.4 Hz; 1.5 nA: 11.2 ± 0.4 Hz; n = 25),with respect to control cells (0.5 nA: 2.3 ± 0.4 Hz; 1.0 nA: 5.7 ± 0.6 Hz; 1.5 nA: 8.6 ± 0.6 Hz; n = 20) (treatment $F_{(1,129)}$ = 33.5, P < 0.0001, stimulus $F_{(3,129)}$ = 312.5, ***P < 0.0001 and interaction $F_{(3,129)}$ = 9.3, P < 0.0001, Repeated Measures ANOVA) (Fig. 4B).

The decreased rheobase and increased MFF could not be related to changes in R_{in} since this was statistically similar between control (52.3 ± 6.3 MΩ, n = 30) and helSynKD cells (67.7 ± 5.7 MΩ, n = 33) (P = 0.07, unpaired t-test).

Analyzing APs fired for each cell, we found that IFF progressively decreased in both control and helSynKD cells (Fig. 4C), and helSynKD cells showed a higher IFF at each interspike interval (ISI) (treatment $F_{(1,124)}$ = 37.5, P < 0.0001, ISI $F_{(2,124)}$ = 13.7, P < 0.0001 and interaction $F_{(2,124)}$ = 0.2, P = 0.80, two-way ANOVA).

Given that spiking decreases in frequency over the 500 ms stimulation, as SFA takes place, we compared the degree of adaptation between control and helSynKD cells (adaptation ratio). In agreement with the faster MFF and higher IFF, helSynKD cells showed a slightly smaller adaptation ratio (1.17 ± 0.02, n = 25) with respect to control cells (1.25 ± 0.03, n = 20) (Welch corrected $t_{(30)}$ = 2.3, P < 0.05) (Fig. 4D).

Adaptation can be associated with the accumulation of inactivated Na^+ and Ca^{2+} channels during the 500 ms stimulation. This accumulation can be reflected in a shift of the V_{th} to more depolarized potentials and the decrease of the maximal rate of velocity (dV/dt_{max}) of each consecutive spike during a sustained stimulation (Colbert et al., 1997; Aidley, 1998; Vandael et al., 2012). Sequential phase plane plot analysis of control and helSynKD cells was used to determine the evolution of V_{th} and dV/dt_{max} during spiking.

The V_{th} of control cells decreased from -22.8 ± 1.2 mV in the first AP to -12.9 ± 3.2 mV in the sixth AP recorded (n = 18), a voltage 45.7% smaller. On the other hand, V_{th} of helSynKD cells decreased from -25.8 ± 1.4 mV in the first AP to -20.0 ± 2.2 mV in the sixth AP (n = 20), a voltage only 25.6% smaller (treatment $F_{(1,174)}$ = 29.6, P < 0.0001, spike $F_{(5,174)}$ = 28.5, P < 0.0001 and interaction $F_{(5,174)}$ = 1.9, P = 0.09, two-way

ANOVA) (Fig. 4E). Although the Em was slightly more depolarized in the helSynKD cells, the stronger AHP observed in these cells (see section 2.2) may account for the reduced accumulation of inactivated channels in the consecutive APs and the reduced value of V_{th}.

Figure 4F shows that the dV/dt_{max} of both control (n = 18) and helSynKD cells (n = 20) markedly decreased between the first and the second AP (around 30%). In the helSynKD cells dV/dt_{max} remained nearly constant during the next APs while it decreased further in control cells. These values however, were not statistically different (treatment $F_{(1,175)} = 3.3$, $P = 0.07$, spike $F_{(5,175)} = 52.2$, $P < 0.0001$ and interaction $F_{(5,175)} = 1.4$, $P = 0.2$, two-way ANOVA). The tendency of dV/dt_{max} to remain high in helSynKD cells is most likely due to the increased AHP that helps to quickly recruit Na^+ and Ca^{2+} channels from inactivation between APs (see below).

2.2. Syn silencing changes the shape of AP waveform

Looking more closely at the AP recordings during current stimulation, the Syn-silenced cells showed remarkable changes of the AP waveform with respect to control cells (Fig. 5A). The most evident variation was the increased fast AHP in helSynKD cells (-5.7 ± 0.7 mV, n = 21), with respect to control cells (-1.2 ± 0.5 mV, n = 21) ($F_{(2,52)} = 15.1$, $P < 0.0001$) (Fig. 5B). In addition, helSynKD cells exhibited a decreased decay time 90%-10% (5.8 ± 0.3 ms, n = 21 in helSynKD cell; vs 10.1 ± 1.1 ms, n = 21 in control cells) ($F_{(2,52)} = 4.6$, $P < 0.05$) (Fig. 5C), but with no statistical significance for the decay time constant (decay tau) (5.1 ± 0.3 ms, n = 21 in helSynKD; vs 5.1 ± 0.4 ms, n = 21 in control cells) ($P = 0.97$, one-way ANOVA) (Fig. 5D) and AP half-width (4.8 ± 0.2 ms, n = 21 in helSynKD; vs 5.1 ± 0.3 ms, n = 21 in control cells) ($P = 0.57$, one-way ANOVA) (Fig. 5E). HelSynKD cells also showed also a slightly lower AP amplitude: 86.4 ± 1.5 mV (n = 21) vs. 92.3 ± 1.5 mV (n = 21) in control cells ($F_{(2.52)} = 4.6$, $P < 0.05$) (Fig. 5F). These results suggest that suppression of Syn mainly influences AP repolarization. Similar decay in the first 63% of the repolarization (decay tau) but decreased decay

90%-10%, with more pronounced fast AHP suggest changes in the final part of the repolarization and probably an increased contribution Ca^{2+}-activated K^+ currents (Storm, 1987; Faber and Sah, 2003; Berkefeld et al., 2010). To test this hypothesis, we bath applied paxilline, a BK channels inhibitor (Zhou and Lingle, 2014) (Fig. 5A, light gray line). In the presence of paxilline the helSynKD cells showed a decreased AHP (-3.5 ± 0.7 mV, n = 11) (Fig. 5B), and a slightly increased decay time 90%-10% (8.1 ± 2.1 ms, n = 11) (Fig. 5C) with respect to values before paxilline addition. In both cases the values measured with paxilline were not statistically different from controls. Decay tau (4.9 ± 0.9 ms, n = 11) (Fig. 5D) and half-width (5.4 ± 0.7 ms, n = 11) (Fig. 5E) were unchanged during paxilline application. In addition, in presence of paxilline there were no significant differences in the AP amplitude between control and helSynKD cells (88.8 ± 0.9 mV, n = 11) (Fig. 5F). Paxilline applied to control cells caused no significant changes to the AP measured parameters (data not shown).

The analysis of the depolarizing phase showed a shorter time to peak in helSynKD cells (31.0 ± 1.9 ms, n = 25) with respect to controls (48.0 ± 4.8 ms, n = 20) (Kruskal-Wallis test = 9.08, P = 0.01) (Fig. 5G), but no statistical difference in the maximum rate of rise of helSynKD cells (46.4 ± 3.3 ms, n = 25) compared to control cells (52.4 ± 4.3 ms, n = 20) (P = 0.56, one-way ANOVA) (Fig. 5H). Addition of paxilline had nearly no effect on any of these parameters in both control and helSynKD cells (data not shown).

2.3. Syn silencing alters Ca^{2+} and BK currents

To test whether the increased AHP is associated with an increased BK current in Syn-silenced cells, we measured the outward K^+ current at different voltages (I-V curve) under voltage-clamp conditions in the presence of Ca^{2+} in the extracellular solution (Fig. 6A). We observed maximal increased K^+ current amplitudes of 60-70% in helSynKD cells (n = 11) compared to control cells (n = 13), particularly at voltages between 0 and 20 mV (treatment $F_{(1,264)} = 4.03$, P = 0.057, potentials $F_{(12,264)} = 264.9$, P < 0.0001 and interaction $F_{(12,264)} = 6.36$, P < 0.0001, Repeated Measures ANOVA) (Fig.

6A and B). Membrane potentials between -30 and 30 mV were used to test BK channel contribution to K^+ currents. Addition of paxilline caused minor changes in K^+ current amplitudes in control cells (Fig 6A and C), while in helSynKD cells the BK channel blocker decreased the K^+ currents amplitude and the I-V curve (open squares in Fig. 6C) became statistically similar to the control I-V curve (filled dots in Fig. 6C) (treatment $F_{(3,210)} = 3.41$, $P < 0.05$, potentials $F_{(6,245)} = 309.9.1$, $P < 0.0001$ and interaction $F_{(18,210)} = 2.84$, $P = 0.0002$, Repeated Measures ANOVA). To estimate the size of BK currents we subtracted the K^+ current traces with paxilline from those without paxilline in control and helSynKD cells (Fig 6D, left panel and insert). The peak values of these traces were plotted against voltage to give the "bell-shaped" I-V curves of Fig 6D (right panel), which are the typical I-V plots of Ca^{2+}-dependent BK currents (treatment $F_{(1,78)} = 1.79$, $P = 0.20$, potentials $F_{(6,78)} = 6.09$, $P < 0.0001$ and interaction $F_{(6,78)} = 2.71$, $P = 0.019$, Repeated Measures ANOVA). Similar "bell-shaped" curves were obtained plotting the steady state values of the traces against voltage (data not showed). The remaining "paxilline-resistant" K^+ currents are effectively carried by voltage-gated K^+ channels whose conductance was calculated and plotted against voltage in Fig. 6E. The solid curves are best fits using Boltzmann equations with half-maximal value (V½) 4.2 mV and slope factor (k) 8.97 mV in control cells and V½= 0 mV and k= 8.97 mV in helSynKD cells. All together these findings indicate that K^+ outward currents in isolated *Helix aspersa* neurons are mainly carried by voltage-gated K^+ channels whose density is not altered by Syn silencing.

In addition, the K^+ I-V relationship supports the former current-clamp observations, pointing towards an increased Ca^{2+}-dependent K^+ current through BK channels in helSynKD cells. We therefore also tested the effect of Syn silencing on the total Ca^{2+} currents in these cells. Whole-cell voltage-clamp recordings were performed to assay the size of inward Ca^{2+} currents (Fig. 7A). At potentials between -20 and +60 mV, we found larger Ca^{2+} current amplitudes in helSynKD cells (n = 11) with respect to control

cells (n = 13) (treatment $F_{(1,308)} = 7.81$, $P < 0.05$, potentials $F_{(14,308)} = 62.79$, $P < 0.0001$ and interaction $F_{(14,308)} = 4.55$, $P < 0.0001$, Repeated Measures ANOVA) (Fig. 7B).

2.4. Effects of BK channels block on firing patterns.

As a final check we tested how BK channels blocked by paxilline besides affecting the waveform of single APs (Fig. 5) and the size of BK currents (Fig. 6), also modify the firing patterns of helSynKD cells (Fig. 8A). Paxilline had nearly no effects on the MFF in control cells (0.5 nA: 3.3 ± 1.0 Hz; 1.0 nA: 5.6 ± 1.5 Hz; 1.5 nA: 8.4 ± 1.0 Hz; n = 9) (not shown), while in helSynKD cells the blocker decreased the MFF to values comparable to control cells (Fig. 8B). This was more evident at stronger stimulations (1.5 nA), reaching a value statistically similar to control value (0.5 nA: 4.7 ± 0.4 Hz; 1.0 nA: 7.5 ± 0.7 Hz; 1.5 nA: 9.5 ± 0.8 Hz; n = 11) (treatment $F_{(3,183)} = 8.9$, $P < 0.0001$, stimulus $F_{(3,183)} = 334.1$, $P < 0.0001$ and interaction $F_{(9,183)} = 4.01$, $P = 0.0001$, Repeated Measures ANOVA).

With 1.5 nA current injection, all parameters associated with the AP firing returned to values similar to controls after helSynKD cells were treated with paxilline (filled dots vs. open triangles in Fig. 8C, E and F). Syn-silenced cells showed slightly decreased IFFs (treatment $F_{(3,171)} = 14.0$, $P < 0.0001$, ISI $F_{(2,171)} = 11.7$, $P < 0.0001$ and interaction $F_{(6,171)} = 0.2$, $P = 0.98$, two-way ANOVA) (Fig. 8C). In addition the adaptation ratio increased (1.3 ± 0.1, n = 10) (Kruskal-Wallis test = 6.25, $P = 0.04$) (Fig. 8D). Despite their strong variation, paxilline treatments increased the voltage threshold of depolarization (V_{th}) of helSynKD cells (n = 11) (treatment $F_{(2,220)} = 18.6$, $P < 0.0001$, spike $F_{(5,220)} = 32.5$, $P < 0.0001$ and interaction $F_{(5,220)} = 1.5$, $P = 0.134$, two-way ANOVA) (Fig. 8E). In addition, the changes in the decay of dV/dt_{max} were not significantly different in helSynKD and control cells; this value decreased towards the last APs, in a similar way that control cells did after paxilline application in helSynKD cells (treatment $F_{(2,220)} = 3.3$, $P < 0.05$, spike $F_{(5,220)} = 68.4$, $P < 0.0001$ and interaction $F_{(10,220)} = 0.8$, $P > 0.05$, two-way ANOVA) (Fig. 8F). Taken together, these data suggest

that BK current elevation is likely the key mechanism regulating the enhanced firing in Syn-silenced cells.

In conclusion, Syn knock-down is associated with an increased cellular excitability that derives from a BK current elevation associated with increased voltage-gated Ca^{2+} currents. Both up-regulations appear to be the key functional change induced by knocking-down Syn in *Helix* neurons that are able to alter the AP firing.

3. Discussion

We studied the changes of cell excitability associated with the constitutive suppression of Syn expression by asRNA in an invertebrate model in order to better understand the epileptic phenotype developed in Syn-deficient organisms. We found that Syn down-regulation in a constitutive way triggers a hyperexcitable state in specific serotonergic neurons isolated from *Helix* land snail, and this enhancement may be associated with increased Ca^{2+} and BK currents.

3.1. Increased cellular excitability in Syn silenced cells.

Almost all single, double or triple Syn KO mice models develop an epileptic phenotype (Li et al., 1995; Rosahl et al., 1995; Gitler et al., 2004; Etholm and Heggelund, 2009; Ketzef et al. 2011; Etholm et al., 2013) and several studies in the literature analyzed the relationship of Syn knock-down and knock-out with epileptogenesis. In addition, epidemiological studies reported several Syn mutations associated with several disorders, such as epilepsy in humans (García et al., 2004; Cavalleri et al., 2007; Lakhan et al., 2010; Fassio et al., 2011b; Lignani et al., 2013; Corradi et al., 2014).

Synaptic transmission of glutamatergic and GABAergic synapses has been studied in Syn-deficient animals and under conditions of Syns down-regulation and deletion, showing an imbalance between excitatory and inhibitory neurotransmission, reducing the GABAergic component and leaving unchanged or increased the glutamatergic component (Terada et al., 1999; Gitler et al., 2004; Baldelli et al., 2007; Chiappalone et al., 2009; Ketzef et al. 2011; Farisello et al., 2012; Medrihan et al., 2013; Feliciano et al., 2013; Lignani et al., 2013; Medrihan et al., 2014), thus leading to an increased network excitability.

Using an organism in which specific neurons can be individually isolated and cultured as single neurons and Syn can be inhibited in a chronic way, we analyzed cell excitability in Syn-deficient neurons in the absence of excitatory or inhibitory inputs and

in absence of possible compensatory mechanisms, in order to explore possible Syn-dependent direct changes in cellular excitability.

Earlier studies reported increased firing rates in neurons from SynI KO mice (Chiappalone et al., 2009), SynII KO mice (Medrihan et al., 2014) and triple KO mice (Farisello et al., 2012), suggesting hyperexcitability in Syn-deficient neurons *in vitro*. In addition, Farisello et al. (2012) reported a depolarized Em and a smaller threshold of AP firing, while Medrihan et al. (2014) reported a slightly depolarized Em, but in this case no statistically significant differences were observed in the threshold of AP firing. These changes in cell excitability were associated with the excitation/inhibition imbalance between glutamatergic and GABAergic synaptic transmission, suggesting that the effects were due, at least in part, to a significant decrease in tonic $GABA_A$ current, decreased asynchronous GABA release and impaired tonic inhibition (Farisello et al., 2012; Medrihan et al., 2014).

It is known that during seizures the increased abnormal activity is dependent not only on the excitatory and inhibitory connections between neurons, but also on the intrinsic properties of each individual cell (Kandel et al., 2013). To better analyze the role of Syn on single cell excitability, we decided to use an invertebrate culture cell preparation that is particularly advantageous since specific identifiable neurons may be isolated from their synaptic inputs and cultured in isolation where they maintain their electrical properties (Ghirardi et al., 1996). In these experiments, serotonergic C1 neurons were isolated from cerebral ganglia of *Helix* snails and kept in culture as floating somata for 3 days following asRNA injections.

The results of our experiments extended former findings and showed that Syn down-regulation in *Helix aspersa* neurons is able to influence intrinsic cell excitability in the absence of excitatory and inhibitory inputs. In agreement with previous results in mice, we showed in this model a slightly depolarized Em, more negative threshold of AP firing and higher firing rates, together with a decreased rheobase and reduced SFA in

Syn-silenced cells with respect to Syn-expressing control cells. Since our cells were cultured isolated of synaptic inputs, the differences between control and helSynKD cells suggest intrinsic changes in cellular excitability when Syn was knocked-down.

As we recently showed (Brenes et al., 2015), helSynKD cells show a faster neurotransmitter release under high frequency stimulation (10 Hz), and this could be associated with a larger RRP. Increased RRPs have also been reported in excitatory synapses of synapsin-deficient mice (Chiappalone et al., 2009; Kile et al., 2011; Farisello et al., 2012). In addition, smaller RRPs have been reported in inhibitory synapses of synapsin-deficient mice (Gitler et al., 2004; Baldelli et al., 2007; Chiappalone et al., 2009; Farisello et al., 2012).

Increased excitability together with larger RRPs in excitatory synapses could be related to an increased excitatory component of the neuronal networks. The combination of increased excitability together with smaller RRPs in inhibitory synapses could generate easily fatigable inhibitory synapses and it could decrease the inhibitory component of the networks.

3.2. Changes in ionic currents.

Increased intrinsic cellular excitability has been reported in epileptic models, usually associated with ionic current modifications (Noebels, 2003). For example, several studies in humans have shown increased BK currents in epilepsy and paroxysmal movement disorders, that correlate with faster cellular spiking behavior (Du et al., 2005; Díez-Sampedro et al., 2006; Lorenz et al., 2007; Shruti et al., 2008; Lee and Cui, 2009; Wang et al., 2009; Yang et al., 2010). However, changes in intrinsic electrical properties of individual cells, as a consequence of Syn silencing and causing increased excitability has not been described yet in the literature.

Searching for a mechanism that links Syn silencing to changes in cell excitability and AP waveforms, we analyzed the effects of Syn silencing on Ca^{2+} and K^{+} currents. Outward K^{+} currents were increased in helSynKD cells, and were composed of a voltage-gated component similar in control and helSynKD cells and a Ca^{2+}-dependent

BK component (Akaike et al., 1983; Hille, 2001) that increased in helSynKD cells. Ca^{2+} currents were also increased in helSynKD cells and this augmentation could drive the increased BK currents observed in Syn-deficient cells. However, we cannot exclude changes of the BK channel expression density in the cell membrane or changes in their subcellular localization. We also did not characterize the type of voltage-gated Ca^{2+} channels specifically up-regulated in helSynKD cells. It is known that *Helix* cells display voltage-gated Ca^{2+} channels type L, N and P/Q (Azanza et al., 2008) and future investigations are planned to identify the specific Ca^{2+} channels affected.

The increased Ca^{2+} permeability could also be related to the slightly decreased resting membrane potential (Condliffe et al., 2010) and the decreased rheobase (Bravo et al., 2011) observed in the neurons in which Syn was silenced. In addition, since AP depolarization in C1 *Helix* neurons depends on Na^{+} and Ca^{2+} channel opening (results not shown), it is possible that the increased Ca^{2+} currents could be associated with the faster depolarization observed in the pre-trigger phase of APs in helSynKD cells.

As far as we know, there are no reports about the changes of Ca^{2+} and Ca^{2+}-dependent BK currents in Syn-deficient cells. However, several studies have suggested that Syn proteins are able to interact with Ca^{2+} channels modifying directly or indirectly their function. Medrihan et al. (2013) showed functional interactions between SynII and presynaptic Ca^{2+} channels (Cav2.1, a P/Q type channel) and an increased ratio of synchronous/asynchronous GABA release. In addition, a potential interaction of SynI and SynII with distinct voltage-gated Ca^{2+} channels has been suggested by proteomic studies (Müller et al., 2010). It has also been reported that SynII KO increases Ca^{2+} sensitivity of release in excitatory transmission (Feliciano et al., 2013).

Our present data do not exclude the possibility that Syn deficiency alters channel kinetics. It is known, in fact, that ion channel/protein interactions can modulate Ca^{2+} channel properties. For instance, knocking-down SNAP-25 results in an increased current density of Cav2.2 (P/Q-type) voltage-gated Ca^{2+} channels, reducing their voltage-dependent inactivation (Condliffe et al., 2010). We also cannot exclude the

possibility that differences in the trafficking of Ca^{2+} and BK channels or their regulatory subunits may contribute to the observed phenomenon. It is known that Syns are involved in actin polymerization and cytoskeleton formation (Cesca et al., 2010), and actin knocking-down could affect trafficking, delivery, segregation, localization, clustering and activity of ion channels. Concerning this issue, it has been reported that cytoskeleton disruption can lead to increased intracellular Ca^{2+} and/or altered regulation of transmembrane ion flux (Janmey, 1998). Several studies have also shown that changes in the actin cytoskeleton dynamics mediate BK channel properties in hippocampal neurons and smooth muscle cells. For instance, actin disruption increases BK channels activation and clustering (O'Malley et al., 2005; O'Malley and Harvey, 2007). Future studies will focus on the changes in channel subcellular localization and channel kinetics in Syn-deprived cells.

As pointed out before, the increased BK currents and their effect on AHP could be related to the faster spiking rates since deeper AHP facilitates sustained high-frequency firing by limiting the accumulation of Na^{+} and Ca^{2+} channel inactivation and by inducing a more rapid channel reactivation following each spike (Mott et al., 1997; Erisir et al., 1999; Faber and Sah, 2003; Fernandez et al., 2005; Shruti et al., 2008; Comunanza et al., 2010; Vandael et al., 2015; Jaffe et al. 2011). Paxilline effect on the MFF during the stronger stimulations suggests that the up-regulation of BK channels could in part enable fast spiking by limiting the channel inactivation during repetitive firing.

Clearly, the larger AHP and the decreased accumulation of inactive channels are not the only factors supporting the fast spiking behavior observed in helSynKD cells. The depolarization phase of the AP in C1 *Helix* neurons is affected by Ca^{2+} channels and Ca^{2+} currents are increased in the Syn-depleted cells. These currents may thus accelerate the depolarization rate at the pre-threshold phase to reach the threshold faster and induce higher frequency firing in Syn-deficient cells.

4. Conclusions

We have shown that Syn knock-down in *Helix* land snail serotonergic neurons is associated with an increased excitability, characterized by decreased Em, lower rheobase, more negative threshold potential and faster spiking frequencies. The APs of the Syn-silenced cells have faster depolarization and repolarization with increased AHP. The changes in the AP waveform and spiking behavior of the helSynKD cells are related to increased Ca^{2+} influx through voltage-gated Ca^{2+} channels and increased Ca^{2+}-dependent BK currents. Although, the specific mechanisms underlying these effects is unknown, the present data clearly suggest an increased intrinsic excitability in cells where Syn is knocked-down, helping to better understand the epileptic phenotype developed in different Syn-deficient organisms. Future studies will assess the specific mechanisms that link Syn knock-down and cell hyperexcitability in this experimental model.

5. Acknowledgements

We thank Carlo Giachello, Daniela Gavello, Virginia Eterno and Adriana Argüello for their technical support and help in the planning, recording or analysis of the experiments; Adarli Romero for helpful comments; and Paul Hanson for language correction.

6. Author's contribution

The experiments included in this study were performed and the manuscript was mainly written by O.B.

D.V., P.G.M., M.G. and E.C. participated to experiment planning, discussion and manuscript correction.

7. Conflict of Interest Statement

Authors disclosed any actual or potential conflict of interest including any financial, personal or other relationships with other people or organizations influencing the present article.

8. References

Aidley D (1998) The physiology of excitable cells. 4th Ed. Cambridge University Press, United Kingdom. 477 pag.

Akaike N, Brown AM, Dahl G, Higashi H, Isenberg G, Tsuda Y, Yatani A (1983) Voltage-dependent activation of potassium currents in Helix neurons by endogenous cellular calcium. J Physiol 334:309-324.

Azanza MJ, Pérez-Castejón C, Pes N, Pérez-Bruzón RN, Aisa J, Junquera C, Maestú C, Lahoz M, Martínez-Ciriano C, Vera-Gil A, Del Moral A (2008) Characterization by immunocytochemistry of ionic channels in *Helix aspersa* suboesophageal brain ganglia neurons. Histol Histopathol 23:397-406.

Baldelli P, Fassio A, Valtorta F, Benfenati F (2007) Lack of synapsin I reduces the readily releasable pool of synaptic vesicles at central inhibitory synapses. J Neurosci 27(49):13520-13531.

Bailey TW, Nicol GD, Schild JH, DiMicco JA (2003) Synaptic and membrane properties of neurons in the dorsomedial hypothalamus. Brain Res 985:150-162.

Berkefeld H, Fakler B, Schulte U (2010) Ca^{2+}-Activated K Channels: From Protein Complexes to Function. Physiol Rev 90:1437-1459.

Bravo-Martínez J, Delgado-Coello B, García DE, Mas-Oliva J (2011) Analysis of plasma membrane Ca^{2+}-ATPase gene expression during epileptogenesis employing single hippocampal CA1 neurons. Exp Biol Med 236:409-417.

Brenes O, Giachello CNG, Corradi AM, Ghirardi M, Montarolo PG (2015) Synapsin knockdown is associated with decreased neurite outgrowth, functional synaptogenesis impairment and, fast high-frequency neurotransmitter release. J Neurosci Res. 93:1492-1506

Cavalleri G, Weale ME, Shianna KV, Singh R, Lynch JM, Grinton B, Szoeke C, Murphy K, Kinirons P, O'Rourke D, Ge D, Depondt C, Claeys KG, Pandolfo M, Gumbs C, Walley N, McNamara J, Mulley JC, Linney KN, Sheffield LJ, Radtke RA, Tate SK,

Chissoe SL, Gibson RA, Hosford D, Stanton A, Graves TD, Hanna MG, Eriksson K, Kantanen AM, Kalviainen R, O'Brien TJ, Sander JW, Duncan JS, Scheffer IE, Berkovic SF, Wood NW, Doherty CP, Delanty N, Sisodiya SM, Goldstein DB (2007) Multicentre search for genetic susceptibility loci in sporadic epilepsy syndrome and seizure types: a case-control study. Lancet Neurol 6:970-780.

Cesca F, Baldelli P, Valtorta F, Benfenati F (2010) The Synapsins: key actors of synapse function and plasticity. Prog Neurobiol 91:313-348.

Chiappalone M, Casagrande S, Tedesco M, Valtorta F, Baldelli P, Martinoia S, Benfenati F (2009) Opposite changes in glutamatergic and GABAergic transmission underlie the diffuse hyperexcitability of synapsin I-deficient cortical networks. Cereb Cortex 19:1422-1439.

Chin LS, Li L, Ferreira A, Kosik KS, Greengard P (1995) Impairment of axonal development and of synaptogenesis in hippocampal neurons of synapsin I-deficient mice. Proc Natl Acad Sci 92:9230-9234.

Colbert CM, Magee JC,Hoffman DA, Johnston D (1997) Slow recovery from inactivation of Na^+ channels underlies the activity-dependent attenuation of dendritic action potentials in hippocampal CA1 pyramidal neurons. J Neurosci 17(17):6512-6521.

Condliffe SB. Corradini I, Pozzi D, Verderio C, Matteoli M (2010) Endogenous SNAP-25 regulates native voltage-gated calcium channels in glutamatergic neurons. J Bio Chem 285:24968-24976.

Comunanza V, Marcantoni A, Vandel D, Mahapatra S, Gavello D, Navarro-Tableros V, Carabelli C, Carbone E (2010) $Ca_v1.3$ as pacemaker channels in adrenal chromaffin cells: Specific role on exo- and endocytosis?. Channels 4(6):440-446.

Corradi A, Fadda M, Piton A, Patry L, Marte A, Rossi P, Cadieux-Dion M, Gauthier J, Lapointe L, Mottron L, Valtorta F, Rouleau GA, Fassio A, Benfenati F, Cossette P (2014) SYN2 is an autism predisposing gene: loss-of-function mutations alter synaptic vesicle cycling and axon outgrowth. Hum Mol Genet 23(1):90-103.

Díez-Sampedro A, Silverman WR, Bautista JF, Richerson GB (2006) Mechanism of increased open probability by mutation of the BK channel. J Neurophysiol 96:1507-1516.

Du W, Bautista JF, Yang H, Díez-Sampedro A, You SA, Wang L, Kotagal P, Lüders HO, Shi J, Cui J, Richerson GB, Wang QK (2005) Calcium-sensitive potassium channelopathy in human epilepsy and paroxysmal movement disorder. Nat genet 37(7):733-738.

Erisir A, Lau D, Rudy B, Leonard S (1999) Function of specific K^+ channels in sustained high-frequency firing of fast-spiking neocortical interneurons. J Neurophysiol 82:2476-2489.

Etholm L, Heggelund P (2009) Seizure elements and seizure element transitions during tonic-clonic seizure activity in the synapsin I/II double knockout mouse: A neuroethological description. Epilepsy Behav 14:582-590.

Etholm L, Bahonjic E, Heggelund P (2013) Sensitive and critical periods in the development of handling induced seizures in mice lacking synapsins: Differences between synapsin I and synapsin II knockouts. Exp Neurol 247:59-65.

Faber ASL, Sah P (2003) Calcium-activated potassium channels: multiple contributions to neuronal function. Neuroscientist 9:181-194.

Farisello P, Boido D, Nieus T, Medrihan L, Cesca F, Valtorta F, Baldelli P, Benfenati F (2012) Synaptic and extrasynaptic origin of the excitation/inhibition imbalance in the hippocampus of synapsin I/II/III knockout mice. Cereb Cortex 23(3):581-593.

Fassio A, Raimondi A, Lignani G, Benfenati F, Baldelli P (2011) Synapsins: From synapse to network hyperexcitability and epilepsy. Semin Cell Dev Biol 22:408-415.

Fassio A, Patry L, Congia S, Onofri F, Piton A, Gauthier J, Pozzi D, Messa M, Defranchi E, Fadda M, Corradi A, Baldelli P, Lapointe L, St-Onge J, Meloche C, Mottron L, Valtorta F, Nguyen DK, Rouleau GA, Benfenati F, Cossette P (2011)

SYN1 loss-of-function mutations in autism and partial epilepsy cause impaired synaptic function. Hum Mol Genet 20(12):2297-2307.

Feliciano P, Andrade R, Bykhovskaia M (2013) Synapsin II and Rab3a cooperate in the regulation of epileptic and synaptic activity in the CA1 region of the hippocampus. J Neurosci 33(46):18319-18330.

Feng J, Chi P, Blanpied TA, Xu Y, Magarinos AM, Ferreira A, Takahashi RH, Kao HT, McEwen BS, Ryan TA, Augustine GJ, Greengard P (2002) Regulation of neurotransmitter release by synapsin III. J Neurosci 22(11):4372-4380.

Fernandez FR, Mehaffey WH, Molineux ML, Turner RW (2005) High-threshold K^+ current increases gain by offsetting a frequency-dependent increase in low-threshold K^+ current. J Neurosci 25(2):363-371.

Ferreira A, Kosik KS, Greengard P, Han HQ (1994) Aberrant neurites and synaptic vesicle protein deficiency in synapsin II-depleted neurons. Science 264:977-979.

Ferreira A, Chin LS, Li L, Lanier LM, Kosik KS, Greengard P (1998) Distinct roles of synapsin I and synapsin II during neuronal development. Mol Med 4:22-28.

Fiumara F, Onofri F, Benfenati F, Montarolo PG, Ghirardi M (2001) Intracellular injection of synapsin I induces neurotransmitter release in C1 neurons of *Helix pomatia* contacting a wrong target. Neuroscience 104(1):271-280.

Fiumara F, Leitinger G, Milanese C, Montarolo PG, Ghirardi M (2005) In vitro formation and activity-dependent plasticity of synapses between Helix neurons involved in the neural control of feeding and withdrawal behaviors. Neuroscience 134:1133-1151.

Fiumara F, Milanese C, Corradi A, Giovedi S., Leitinger G., Menegon A., Montarolo PG, Benfenati F, Ghirardi M (2007) Phosphorylation of synapsin domain A is required for post-tetanic potentiation. J Cell Sci 120:3228-3237.

Gaffield MA, Betz WJ (2007) Synaptic vesicles mobility in mouse motor nerve terminals with and without synapsin. J Neurosci 27(50):13691-13700.

Garcia CC, Blair HJ, Seager M, Coulthard A, Tennant S, Buddles M, Curtis A, Goodship JA (2004) Identification of a mutation in synapsin I, a synaptic vesicle protein, in a family with epilepsy. J Med Genet 41:183-186.

Ghirardi M, Casadio A, Santarelli L, Montarolo PG (1996) Aplysia hemolymph promotes neurite outgrowth and synaptogenesis of identified Helix neurons in cell culture. Invertebrate Neurosci 2:41-49.

Giannandrea M, Guarnieri FC, Genhring NH, Monzani E, Benfenati F, Kulozik AE, Valtorta F (2013) Nonsense-mediated mRNA decay and loss-of-function of the protein underlie the X-linked epilepsy associated with the W356X mutation in synapsin I. PLOS ONE: 8(6): e67724. doi: 10.1371/journal.pone.0067724

Gitler D, Takagishi Y, Feng J, Ren Y, Rodriguez RM, Wetsel WC, Greengard P, Augustine GJ (2004) Different presynaptic roles of synapsins at excitatory and inhibitory synapses. J Neurosci 24:11368-11380.

Hille B (2001) Ion channels of excitable membranes. 3rd edition. Sinauer Associates Inc, USA. 814 pag.

Humeau Y, Doussau F, Vitiello F, Greengard P, Benfenati F, Poulain B (2001) Synapsin controls both reserve and releasable synaptic vesicle pools during neuronal activity and short-term plasticity in Aplysia. J Neurosci 21(12):4195-4206.

Jaffe DB, Wang B, Brenner R (2011) Shaping of action potentials by type I and type II large-conductance Ca^{2+}-activated K^{+} channels. Neuroscience 192:205-218.

Janmey PA (1998). The cytoskeleton and cell signaling: component localization and mechanical coupling. Physiol Rev 78(3):763-781.

Jenerick H (1963) Phase plane trajectories of the muscle spike potential. Biophys J 3:363-377.

Kandel ER, Schwartz JH, Jessell TM, Siegelbaum SA, Hudspeth AJ (2013) Principles of neural science. 5th ed. McGraw Hill, USA.1709 pag.

Kao HT, Song HJ, Porton B, Ming GL, Hoh J, Abraham M, Czernik AJ, Pieribone VA, Poo MM, Greengard P (2002) A protein kinase A-dependent molecular switch in synapsin regulates neurite outgrowth. Nat neurosci 5(5):431-437.

Kile BM, Guillot TS, Venton BJ, Wetsel WC, Augustine GJ, Wightman RM (2010) Synapsins differentially control dopamine and serotonin release. J Neurosci 30(29):9762-9770.

Ketzef M, Kahn J, Weissberg I, Becker AJ, Friedman A, Gitler D (2011) Compensatory network alterations upon onset of epilepsy in sunapsin triple knock-out mice. Neuroscience 189:108-122.

Lakhan R, Kalita J, Kumari R, Mittal B (2010) Association of intronic polymorphism rs3773364 A>G in synapsin-2 gene with idiopathic epilepsy. Synapse 64:403-408.

Lee US, Cui J (2009) β subunit-specific modulations of BK channel function by a mutation associated with epilepsy and dyskinesia. J Physiol 587(7):1481-1498.

Li L, Chin LS, Shupliakov O, Brodin L, Sihra TS, Hvalby O, Jensen V, Zheng D, McNamara JO, Greengard P (1995) Impairment of synaptic vesicle clustering and of synaptic transmission, and increased seizure propensity, in synapsin I-deficient mice. Proc Natl Acad Sci 92:9235-9239.

Lignani G, Raimondi A, Ferrea E, Rocchi A, Paonessa F, Cesca F, Orlando M, Tkatch T, Valtorta F, Cossette P, Baldelli P, Benfenati F (2013) Epileptogenic Q555X SYN1 mutant triggers imbalances in release dynamics and short-term plasticity. Hum Mol Genet 22(11):2186-2199.

Lorenz S, Heil A, Kasper JM, Sander T (2007) Allelic association of a truncation mutation of the KCNMB3 gene with idiopathic generalized epilepsy. Am J Med Genet 144B:10-13.

Marcantoni A, Carabelli V, Vandael DH, Comunanza V, Carbone E (2009) PDE type-4 inhibition increases L-type Ca^{2+} currents, action potential firing, and quantal size of

exocytosis in mouse chromaffin cells. Pflügers Archiv-European J Physiol 457:1093-1110.

Marcantoni A, Vandael DHF, Mahapatra S, Carabelli V, Sinnegger-Brauns MJ, Striessnig J, Carbone E (2010) Loss of Cav1.3 Channels Reveals the Critical Role of L-Type and BK Channel Coupling in Pacemaking Mouse Adrenal Chromaffin Cells. J Neurosci 30:491-504.

Medrihan L, Cesca F, Raimondi A, Lignani G, Baldelli P, Benfenati F (2013) Synapsin II desynchronizes neurotransmitter release at inhibitory synapses by interacting with presynaptic calcium channels. Nature Comm 4:1512.

Medrihan L, Ferrea E, Greco B, Baldelli P, Benfenati F (2014). Asynchronous GABA release is a key determinant of tonic inhibition and controls neuronal excitability: a study in the synapsin $II^{-/-}$ mouse. Cereb cortex doi: 10.1093/cercor/bhu141

Messa M, Congia S, Defranchi E, Valtorta F, Fassio A, Onofri F, Benfenati F (2010) Tyrosine phosphorylation of synapsin I by Src regulates synaptic-vesicle trafficking. J cell Sci 123(13):2256-2268.

Mott DD, Turner DA, Okazaki MM, Lewis DV (1997) Interneurons of the dentate–hilus border of the rat dentate gyrus: morphological and electrophysiological heterogeneity. J Neurosci 17(11):3990-4005.

Müller CS, Haupt A, Bildl W, Schindler J, KnausH-G, MeissnerM, Rammner B, Striessnig J, Flockerzi V, Fakler B, Schulte U (2010) Quantitative proteomics of the Cav2 channel nano-environments in the mammalian brain. Proc Natl Acad Sci 107(34):14950-14957.

Noebels JL (2003) The biology of epilepsy genes. Annu Rev Neurosci 26:599-625.

Noebels JL, Avoli M, Rogawski R, Olsen R, Delgado-Escueta AV (2010) Jasper's Basic Mechanisms of the Epilepsies'' Workshop. Epilepsia 51(Suppl. 5):1–5.

O'Malley D, Irving AJ, Harvey J (2005) Leptin-induced dynamic changes in the actin cytoskeleton mediate the activation and synaptic clustering of BK channels. FASEB J 19(13):1917-1939.

O'Malley D, Harvey J (2007) MAPK-dependent actin cytoskeletal reorganization underlies BK channel activation by insulin. Eur J Neurosci 25:673-682.

Orenbuch A, Shalev L, Marra V, Sinai I, Lavy Y, Kahn J, Burden JJ, Staras K, Gitler D (2012) Synapsin selectively controls the mobility of resting pool vesicles at hippocampal terminals. J Neurosci 32(12):3969-3980.

Pitkänen A, Lukasiuk K (2011) Mechanisms of epileptogenesis and potential treatment targets. The lancet 10:173-186.

Rosahl TW, Spillane D, Missler M, Herz J, Selig DK, Wolff JR, Hammer RE, Malenka RC, Sudhof TC (1995). Essential functions of synapsin-I and synapsin-II in synaptic vesicle regulation. Nature 375:488-493.

Shruti S, Clem RL, Barth AL (2008) A seizure-induced gain-of-function in BK channels is associated with elevated firing activity in neocortical pyramidal neurons. Neurobiol Dis 30(3):323-330.

Soto E, Salceda E, Cruz R, Ortega A, Vega R (2000) Microcomputer program for automated action potential waveform analysis. Comput Methods Programs Biomed 62:141-144.

Storm JF (1987) Action potential repolarization and a fast after-hyperpolarization in rat hippocampal pyramidal cells. J Physiol 385:733-759.

Terada S, Tsijumoto T, Takei Y, Takahashi T, Hirokawa N (1999) Impairment of inhibitory synaptic transmission in mice lacking synapsin I. J Cell Bio 145(5):1039-1048.

Valtorta F, Pozzi D, Benfenati F, Fornasiero EF (2011) The synapsins: Multitask modulators of neuronal development. Semin Cell Dev Biol 22:378-386.

Vandael DHF, Zuccotti A, Striessnig J, Carbone E (2012) CaV1.3-driven SK channel activation regulates pacemaking and spike frequency adaptation in mouse chromaffin cells. J Neurosci 32(46):16345-16359.

Vandael DH, Ottaviani MM, Legros C, Lefort C, Guerineau NC, Allio A, Carabelli V, Carbone E (2015) Reduced availability of voltage-gated sodium channels by

depolarization or blockade by tetrodotoxin boosts burst firing and catecholamine release in mouse chromaffin cells. J Physiol 593:905-927.

Verstegen AMJ, Tagliatti E, Lignani G, Marte A, Stolero T, Atias M, Corradi A, Valtorta F, Gitler D, Onofri F, Fassio A, Benfenati F (2014) Phosphorylation of synapsin I by cyclin-dependent kinase-5 sets the ratio between the resting and recycling pools of synaptic vesicles at hippocampal synapses. J Neurosci 34(21):7266-7280.

Wang B, Rothberg BS, Brenner R (2009) Mechanism of increased BK channel activation from a channel mutation that causes epilepsy. J Gen Physiol 133(3):283-294.

Yang J, Krishnamoorthy G, Saxena A, Zhang G, Shi J, Yang H, Delaloye K, Sept D, Cui J (2010) An epilepsy/dyskinesia-associated mutation enhances BK channel activation by potentiating Ca^{2+} sensing. Neuron 66:871-883.

Zhou Y, Lingle CJ (2014) Paxilline inhibits BK channels by an almost exclusively closed-channel block mechanism. J Gen Physiol 144:415-440.

9. Figure legends

Figure 1. Action potential measurements. Image representation of the action potential (AP) parameters measured for waveform characterization. We measured the resting membrane potential (Em), the time between stimulus and AP peak (time to peak), the voltage threshold for AP firing (V_{th}), the AP amplitude from Em, the AP width at half amplitude (Half-width), the decay time of the first 63% of total repolarization (decay tau), the decay time between the 90 and 10% of the repolarization (Decay time 90-10%), and the after-hyperpolarization (AHP).

Figure 2. *Helix* synapsin knock-down. A. Representative images from immunocytochemistry analysis with a custom antibody against *Helix* synapsin (helSyn) in a control and a synapsin-silenced cell (helSynKD) after 48 h of asRNA expression. Scale bar: 5 µm. B. Fluorescence intensity in arbitrary units (A.U.) of the varicosities selected in A and of their proximal neurites, corrected against their neighboring background.

Figure 3. Increased cellular excitability in synapsin knock-down cells (helSynKD). Excitability was estimated by different means. Measuring the resting membrane potential (Em) (A), the minimal current injection intensity necessary to evoke an action potential (rheobase) (B), and the voltage threshold (V_{th}) for action potential firing (C). In C, the phase plane plot analysis (dV/dt vs. V) of averaged action potentials was used to calculate V_{th} (dashed lines) and mean values are showed as an insert. Each bar indicates the mean ± s.e.m. * $P < 0.05$, ** $P < 0.01$, *** $P < 0.0001$.

Figure 4. Increased firing in synapsin knock-down cells (helSynKD). A. Representative recordings of control and helSynKD cell action potentials, aligned for a better appreciation. B. Mean firing frequency (MFF) plotted as a function of the injected current. Instantaneous firing frequency (IFF) at each interspike interval (ISI) (C), and

the corresponding adaptation ratio (D), were measured during the 1.5 nA stimulation. Voltage threshold (V_{th}) (E) and the maximal depolarization velocity (dV/dt_{max}) (F) were also measured for each spike fired during the 1.5 nA stimulation. Each value indicates the mean ± s.e.m. * P < 0.05, ** P < 0.01, *** P < 0.0001.

Figure 5. Synapsin down-regulation was associated with changes in action potential waveform, in part dependent on BK channels. A. Representative trace of action potentials (AP) in control cells and in synapsin–silenced cells (helSynKD) in presence (+ paxi) or absence (- paxi) of paxilline. In the three conditions we measured after-hyperpolarization (AHP) amplitude (B), decay time between the 90% and the 10 % of the repolarization phase (C), decay time constant (decay tau) (D), AP half-width (E), and AP amplitude (F). Time to peak (G) and maximum rise slope (H) were also measured. Paxilline effects on control cells and on depolarization values are nor shown. Each bar indicates the mean ± s.e.m. * P < 0.05, ** P < 0.01, *** P < 0.0001.

Figure 6. BK and voltage-gated K^+ currents in control and helSynKD cells. A. Representative K^+ currents before and after paxilline addition in control and helSynKD cells recorded at the indicated potentials. B. I-V relationship of the K^+ outward currents in control and helSynKD cells. C. Effect of paxilline on K^+ currents at voltages between -30 and 30 mV. Each data value is the mean ± s.e.m. D. On the left panel, representative K^+ currents at 10 mV obtained before (black) and after (gray) paxilline addition and the “paxilline-sensitive” BK component obtained by subtracting the two traces (see insert) and on the right panel the I-V relationship of the maximal BK current amplitude. Notice the typical “bell-shaped” I-V curve representative of BK currents. E. Residual “paxilline-resistant” voltage-gated K^+ channel conductance versus voltage in control and in helSynKD cells were calculated and fitted by Boltzmann equations as described in the text. Notice the steep voltage-dependence of both I-V curves. * P < 0.05, ** P < 0.01, *** P < 0.001.

Figure 7. Increased Ca^{2+} currents in helSynKD cells. A. Representative Ca^{2+} currents. B. Ca^{2+} currents measured at different voltage steps (I-V relation) in control and synapsin-silenced cells (helSynKD). Each value indicates the mean ± s.e.m. *** P < 0.001.

Figure 8. BK channels influence cell firing in a stimulus intensity-dependent way in synapsin-silenced cells (helSynKD) by affecting channel recovery. A. Representative traces of the effect of paxilline treatment on firing behavior of helSynKD cells with respect to control cells. B. Mean firing frequency (MFF) in control cells and in helSynKD cells in absence and presence of paxilline. Instantaneous firing frequency (IFF) at each interspike interval (ISI) in helSynKD cells (C) and adaptation ratio (D) in absence (- paxi) and presence (+ paxi) of paxilline. Changes in the V_{th} and dV/dt_{max} of each action potential in the 500 ms stimulation at 1.5 nA (E and F, respectively) are presented as the % regarding the first AP of each stimulation in presence and absence of paxilline. Each value indicates the mean ± s.e.m. * P < 0.05, ** P < 0.01, *** P < 0.001 in helSynKD with respect to control cells and $^{++}$ P < 0.01, helSynKD + Paxilline with respect to control cells.

Fig. 1

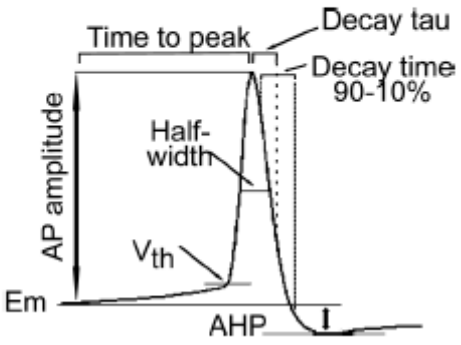
Time to peak
Decay tau
Decay time
90-10%
AP amplitude
Half-
width
V_{th}
Em
AHP

Fig. 2

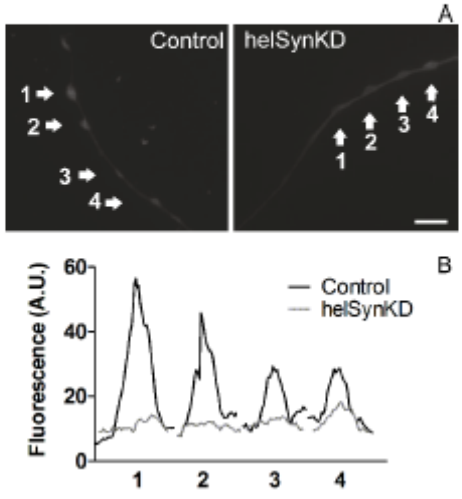
A
Control
helSynKD
1
2
3
4
1
2
3
4
B
Control
helSynKD
Fluorescence (A.U.)
60
40
20
0
1
2
3
4

Fig. 3

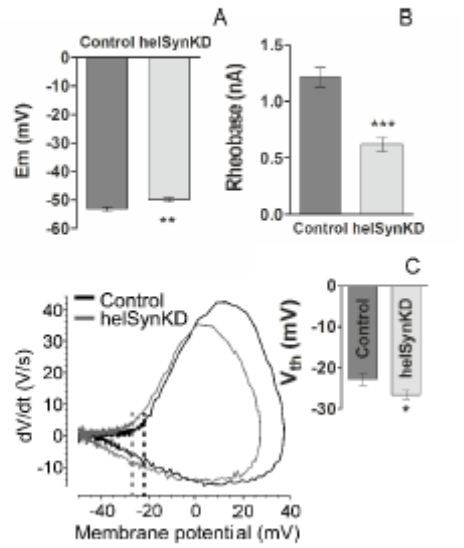
A
Control helSynKD
Em (mV)
0
-10
-20
-30
-40
-50
-60
**
B
Rheobase (nA)
1.5
1.0
0.5
0.0
***
Control helSynKD
C
Control
helSynKD
dV/dt (V/s)
40
30
20
10
0
-10
-40 -20 0 20 40
Membrane potential (mV)
V_{th} (mV)
0
-10
-20
-30
Control
helSynKD
*

Fig. 4

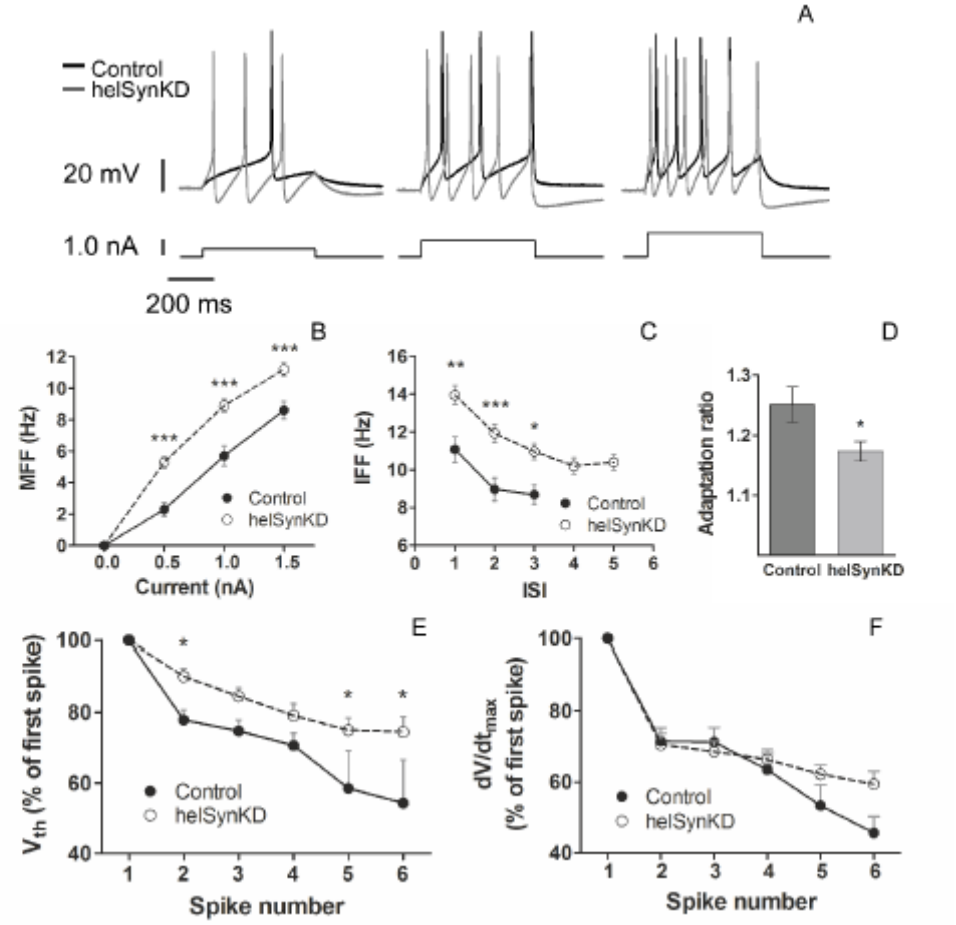
A
Control
helSynKD
20 mV
1.0 nA
200 ms
B
MFF (Hz)
12
10
8
6
4
2
0
***
***
***
Control
helSynKD
0.0 0.5 1.0 1.5
Current (nA)
C
IFF (Hz)
16
14
12
10
8
6
**
***
*
Control
helSynKD
0 1 2 3 4 5 6
ISI
D
Adaptation ratio
1.3
1.2
1.1
*
Control helSynKD
E
V_{th} (% of first spike)
100
80
60
40
*
* *
Control
helSynKD
1 2 3 4 5 6
Spike number
F
dV/dt_{max} (% of first spike)
100
80
60
40
Control
helSynKD
1 2 3 4 5 6
Spike number

Fig. 5

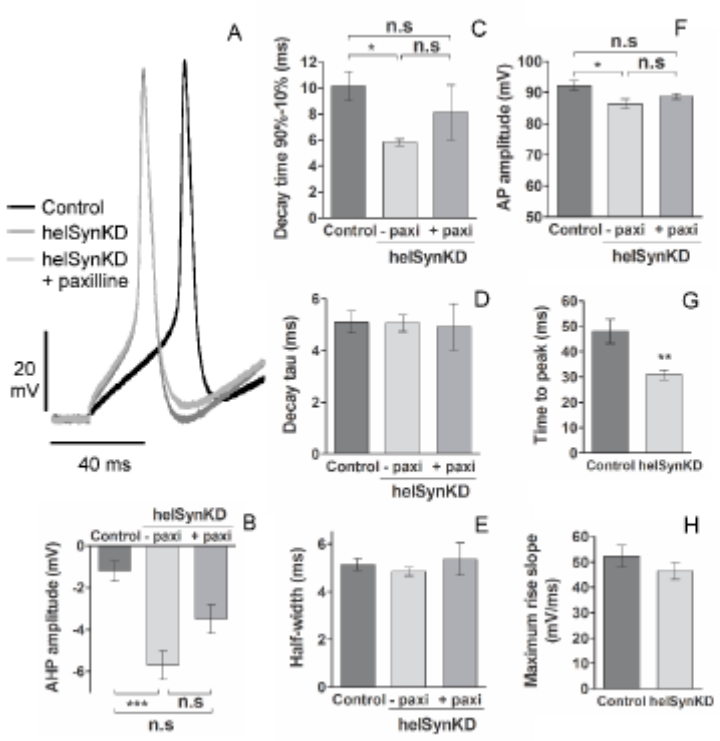
A
Control
helSynKD
helSynKD
+ paxilline
20
mV
40 ms
B
helSynKD
Control - paxi + paxi
AHP amplitude (mV)
***
n.s
n.s
C
n.s
*
n.s
Decay time 90%-10% (ms)
Control - paxi + paxi
helSynKD
D
Decay tau (ms)
Control - paxi + paxi
helSynKD
E
Half-width (ms)
Control - paxi + paxi
helSynKD
F
n.s
*
n.s
AP amplitude (mV)
Control - paxi + paxi
helSynKD
G
Time to peak (ms)
**
Control helSynKD
H
Maximum rise slope (mV/ms)
Control helSynKD

Fig. 6

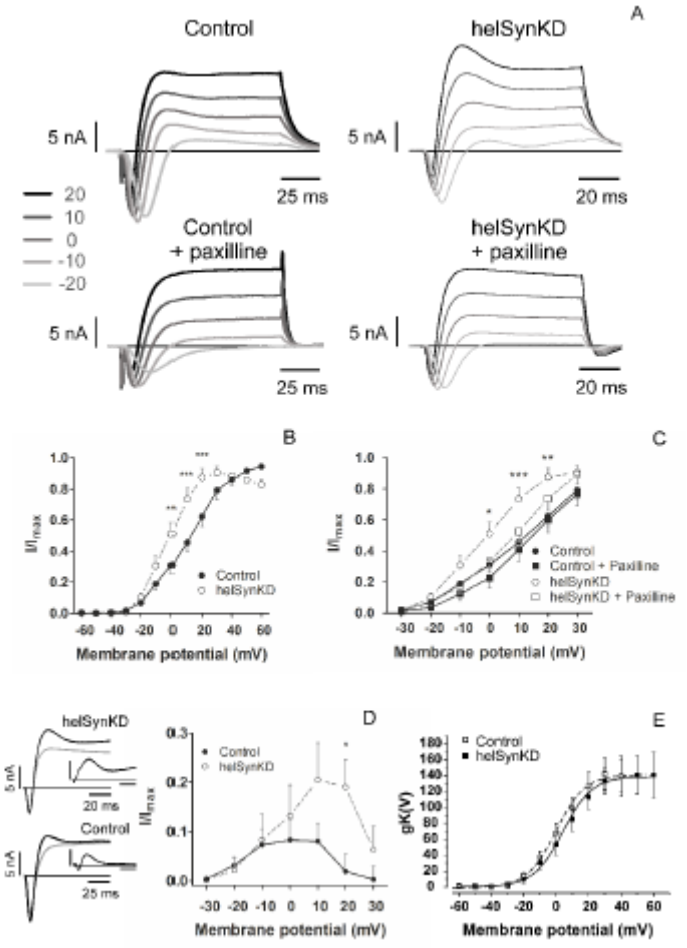
A
Control
helSynKD
5 nA
25 ms
20 ms
20
10
0
-10
-20
Control
+ paxilline
helSynKD
+ paxilline
B
C
I/I max
Membrane potential (mV)
Control
helSynKD
Control + Paxilline
helSynKD + Paxilline
D
E
gK(V)

Fig. 7

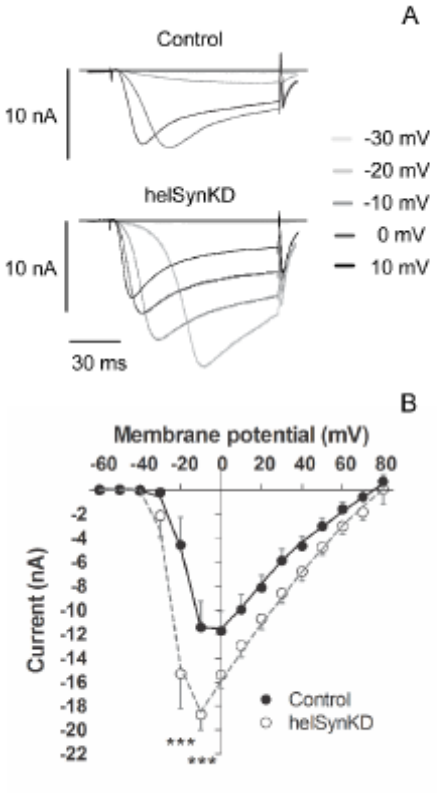
A
Control
10 nA
helSynKD
10 nA
30 ms
-30 mV
-20 mV
-10 mV
0 mV
10 mV
B
Membrane potential (mV)
-60 -40 -20 0 20 40 60 80
Current (nA)
-2 -4 -6 -8 -10 -12 -14 -16 -18 -20 -22
Control
helSynKD
***
***

Fig. 8

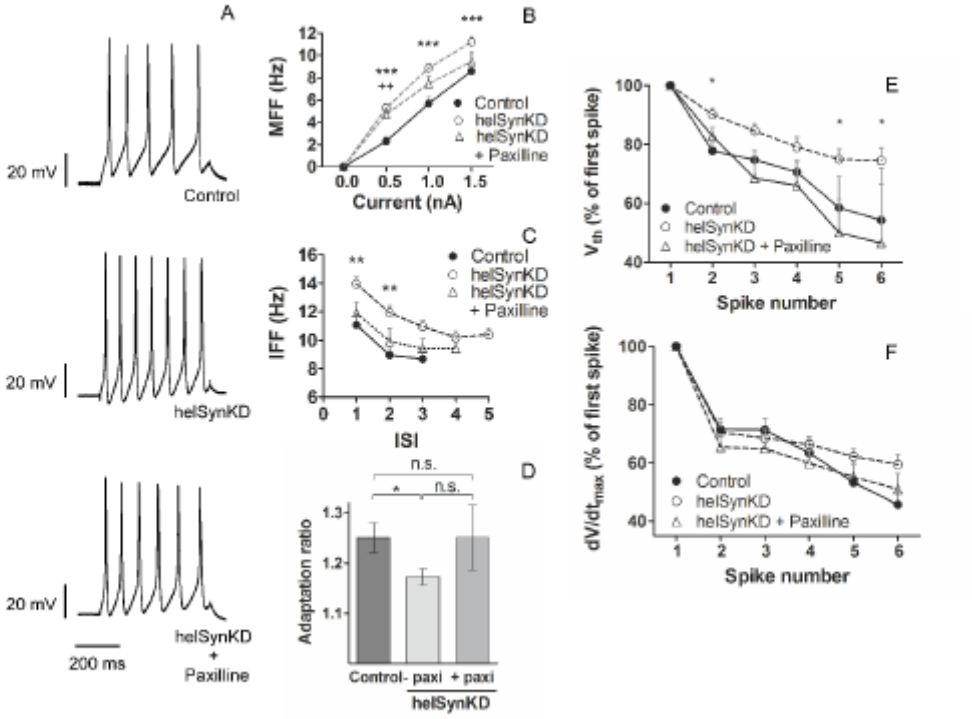
A
20 mV
Control
20 mV
helSynKD
20 mV
200 ms
helSynKD
+
Paxilline
B
MFF (Hz)
Current (nA)
Control
helSynKD
helSynKD
+ Paxilline
C
IFF (Hz)
ISI
D
Adaptation ratio
n.s.
n.s.
Control- paxi + paxi
helSynKD
E
Vth (% of first spike)
Spike number
F
dV/dtmax (% of first spike)
Spike number